

# Study of the microstructure and mechanical properties of a TiCu-based alloy produced by vacuum casting with rapid cooling

*Xianzhang Feng<sup>1</sup>, Haihang Wang<sup>1</sup>, Xinfang Zhang<sup>2</sup>, Junwei Cheng<sup>2</sup>, Tao Hou<sup>3</sup>*

<sup>1</sup>School of Aeronautical Engineering, Zhengzhou University of Aeronautics, Zhengzhou, Henan, P.R. China, 450046

<sup>2</sup>School of Materials Science and Engineering, Zhengzhou University of Aeronautics, Zhengzhou, Henan, P.R. China, 450046

<sup>3</sup>Hebi City Special Equipment Inspection Institute, Henan, P.R. China, 458030

*Received January 25, 2024*

The microstructure of the TiCu alloy obtained by solidification by vacuum casting into a copper mold was studied for observation and imaging of tissues. Research was carried out using optical microscopy, scanning electron microscopy and transmission electron microscopy. Studies have shown that upon rapid cooling of TiCu-based alloys, martensitic structures are formed, which are embedded in  $\gamma$ -TiCu and TiCu. They effectively counteract local shear stress, which leads to rotational diffusion and an increase in shear bands. This prevents the propagation of microcracks caused by excessive local stress during deformation. Research results show that it can effectively improve the microstructure and mechanical properties of alloys based on TiCu.

**Keywords:** TiCu based alloy, rapid solidification, rapid cooling, microstructure, martensite.

**Дослідження мікроструктури та механічних властивостей сплаву на основі TiCu, отриманого методом вакуумного лиття при швидкому охолодженні.**  
*Xianzhang Feng, Haihang Wang, Xinfang Zhang, Junwei Cheng, Tao Hou*

Досліджено мікроструктуру сплаву TiCu отриманого методом затвердіння шляхом вакуумного лиття в мідну форму для спостереження та отримання зображень тканин. Дослідження проведені за допомогою оптичної мікроскопії, скануючої електронної мікроскопії та електронної мікроскопії, що просвічує. Дослідження показали, що при швидкому охолодженні в сплавах на основі TiCu відбувається утворення мартенситних структур, які впроваджуються в  $\gamma$ -TiCu та TiCu. Вони ефективно протидіють локальній зсувній напрузі, що призводить до обертальної дифузії, збільшення смуг зсуву. Це перешкоджає поширенню мікротріщин, спричинених надмірною локальною напругою під час деформації. Результати досліджень показують, що це може ефективно покращити мікроструктуру та механічні властивості. сплавів з урахуванням TiCu.

## **1 Introduction**

Titanium alloy is an alloy consisting of titanium as a base and other added elements. Titanium has two types of homogeneous and heterogeneous crystals:  $\alpha$ -Ti with a close-packed hexagonal structure at temperatures below 882°C

and  $\beta$ -Ti with a body-centered cubic structure at temperatures above 882°C. Rapid solidification makes it possible to increase the solubility of metals in the liquid state, change the density of the material, make different parts of the material more compact, change the proportions of various elements in the metal and thereby

change the properties of the material to meet the requirements of a specific purpose.[1-3]

Due to the higher solidification speed compared to conventional casting, the resulting solidification crystals are smaller and the grain distribution is more uniform, which to some extent reduces the mixing of impurities and improves the quality of the material, thereby giving it high strength. The titanium alloy obtained after processing has excellent mechanical properties, so titanium alloys are used in many fields.[4-9]

Using rapid solidification/powder metallurgy technology, McDonnell Douglas in the United States has successfully developed a high density, high-purity titanium alloy with strength equivalent to that of titanium alloys currently used at room temperature at 760 °C[10-12].

This article mainly focuses on the observation of the microstructure of  $Ti_{50}Cu_{50}$  alloy under rapid solidification and the study of its mechanical properties. The use of copper mold suction casting method to obtain  $Ti_{50}Cu_{50}$  alloy specimens and bars, and the study of their microstructure and mechanical properties, have a good reference value for future research of amorphous nanomaterials [13-19].

## 2. Experimental materials and methods

### 2.1 Experimental equipment

In order to investigate whether the as cast samples were subjected to energy dispersive X-ray after compression testing, a Philips CM200 transmission electron microscope was used for analysis. The TEM samples were prepared by conventional methods of slicing and grinding. At a heating rate of 20 K/m, a Lindeis DTA 1600 differential thermal analyzer was used in this experiment to determine the phase composition and phase transition rate during the heating process.

### 2.2 Material preparation

Vacuum suction casting is used to manufacture large samples. The setting of the copper mold vacuum suction casting equipment is shown in Figure 1. The casting is placed on a copper crucible with a small fully connected water-cooled copper mold. It is empty inside and filled with high concentration argon gas multiple times. The casting is melted by an arc in an argon atmosphere of 0.08 MPa and maintains a certain degree of overheating. The suction valve is opened and connected to the

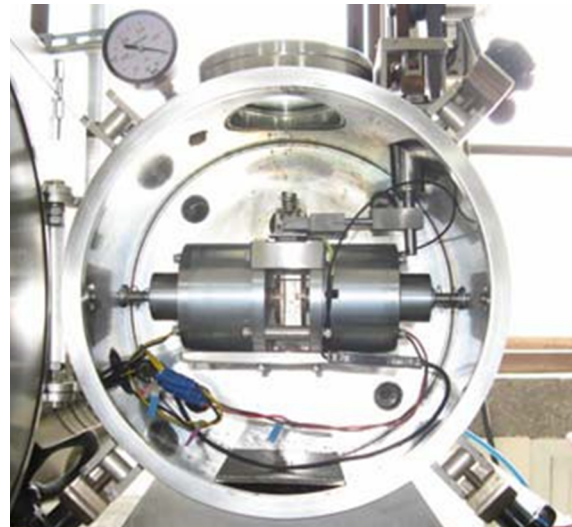


Fig 1. Copper mold vacuum casting equipment

low-voltage cabinet, while turning off the arc power supply, and suck the melted ingot into the water-cooled copper mold to obtain the required sample.

## 3. Results and discussion

### 3.1 Material microstructure analysis

The  $Ti_{50}Cu_{50}$  specimen rod belongs to a special component in the Ti-Cu binary alloy system. The composite Ti-Cu (48-52 at% Cu) uniformly melts at 1248 K, and is slightly enriched in Ti (50.7 at %). The temperature drops to room temperature and remains stable. But the ratio of components has been reduced to near  $Ti_{50}Cu_{50}$ . Due to the chemical similarity between titanium and zirconium, the martensitic transformation of the  $Ti_{50}Cu_{50}$  alloy in the cast state is of engineering importance.

The measured full half width limit (FHWM) of X-ray diffraction peaks is quite broad, approximately  $2\theta = 4^\circ$  in Figure 2 (a). The optical micrograph in Figure 2(b) shows clear linear contrast and a network typical of a martensitic microstructure.

Therefore, the broad diffraction lines in Figure 2(a) can be considered to be due to the internal deformation caused by the local martensitic transformation of the TiCu phase during the solidification process.

### 3.2 DTA Results

In Figure 2, due to the limited resolution of the X-ray diffraction pattern, some phases cannot be detected due to their low content. Therefore, DTA was chosen to detect the phase com-

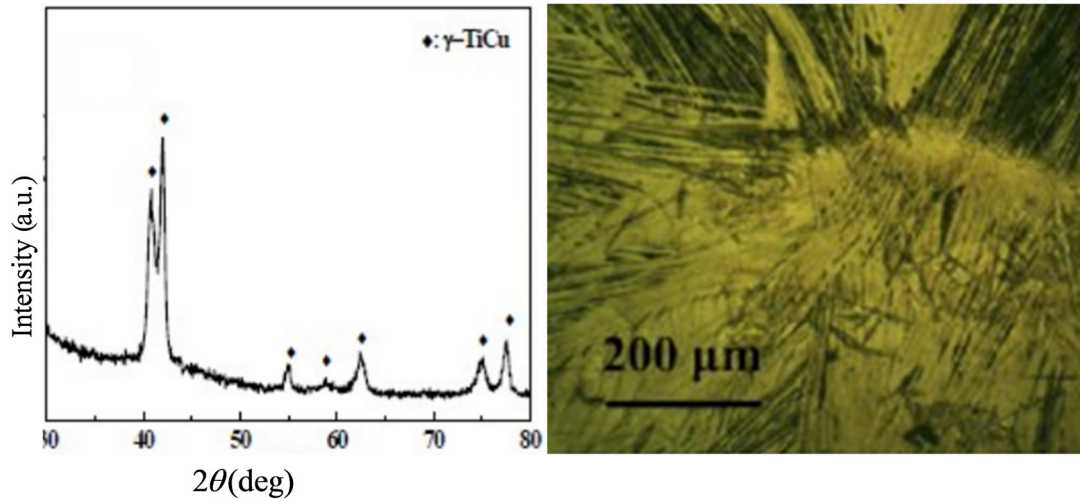


Fig 2. Metallographic structure of Ti-Cu alloy cast rod

position and phase transitions during the heating process of the cast  $\text{Ti}_{50}\text{Cu}_{50}$  alloy (Fig. 3).

According to the Ti-Cu binary phase diagram, the main peak corresponds to  $\gamma$ -TiCu melt, which is consistent with the XRD results. At the lower temperature, the corresponding mother phase (B2) transforms into  $\beta$ -Ti(Cu). The smaller peak corresponds to the endothermic process of transition of the copper Ti (Cu) solid solution into the  $\beta$ -Ti (Cu) solid solution. Through phase separation, B2 may transform into a liquid metal  $\beta$ -Ti solid solution; it transforms into B19 martensite during rapid cooling. Figure 3 shows that upon rapid solidification, the  $\text{Ti}_{50}\text{Cu}_{50}$  rod with a diameter of 2 mm consists of the micrometer-scale B19 martensitic phase  $\gamma$ -TiCu.

### 3.3 Mechanical behavior analysis

The stress-strain curve of Ti-Cu alloy cast rods under compression at room temperature is shown in Figure 4. In the inset, the SEM secondary electron microscopy image of the fractured sample surface is shown.

Fig. 4 shows the secondary electron microscopy (SEM) image of the fractured sample surface after compression at room temperature. The yield stress  $\sigma_y$  and yield strain  $\varepsilon_y$  of as cast bulk  $\text{Ti}_{50}\text{Cu}_{50}$  alloy was measured as 421 MPa and 1.91%, respectively. Ultimate compressive stress  $\sigma_{\max}$  and plastic strain  $\varepsilon_p$  were 1705 MPa, and 18.04%, respectively. During compression, the sample first yields and then fractures after undergoing significant plastic deformation. It can be seen that the sample exhibits a high performance of 18.04%.

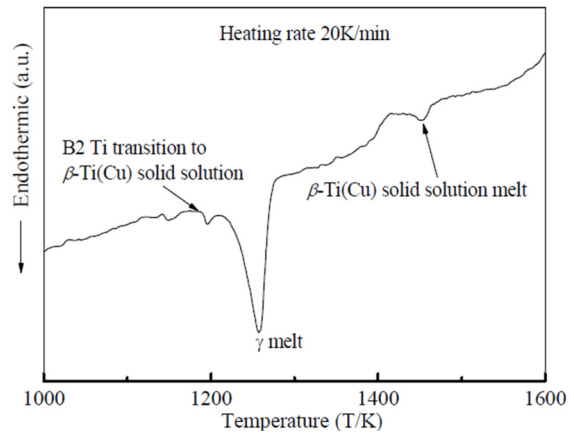


Fig 3. DTA curve of TiCu alloy cast rod

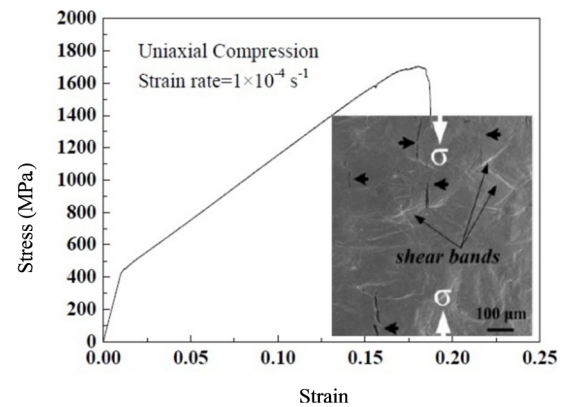


Fig 4. Stress-strain curve and electron microscopic photograph of the surface of a fractured specimen

The secondary electron microscopy image obtained from the surface of the sample under the condition of 15% plastic deformation is shown in Figure 5.

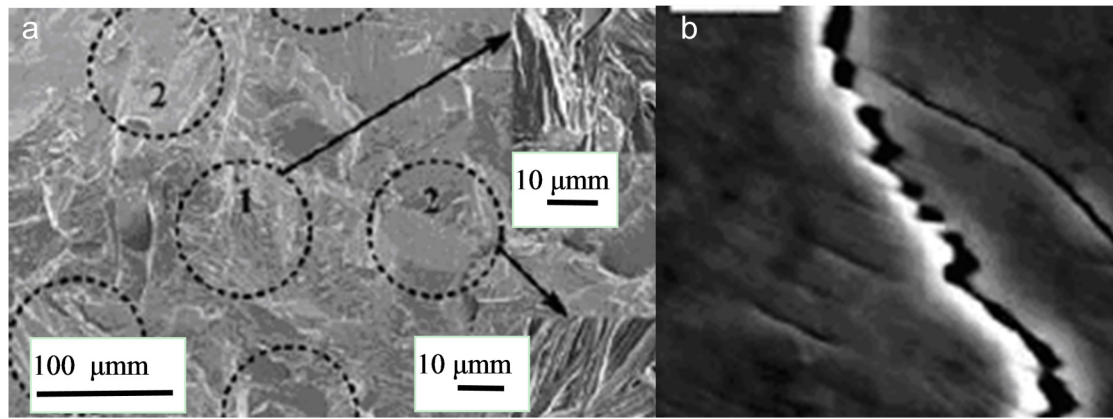


Fig.5 Microscopic view of the sample (a) Microscopic image of fracture surface. (b) Secondary electron microscopy of plastic deformation

The local sample area marked as circle 1 in Figure 5 (a) is parallel to the maximum shear stress surface ( $\tau_{\max}$ ), which is approximately  $45^\circ$  in the direction of pressure; while another local sample area labeled as circle 2 in 5 (a) is parallel to the direction of pressure. The detailed secondary electron microscopy image obtained from Zone 1 in Figure 5 (a) shows that a large number of shear bands exhibit plastic flow in Zone 1. On the other hand, the detailed SEM micrographs obtained from Zone 1 demonstrate typical brittle fracture surfaces and the growth of microcracks, which can often be seen from the metallographic examination. The propagation of microcracks is blocked by a cast state network of martensite without obvious plastic flow. Therefore, it can be considered that the propagation of shear bands in  $\text{Ti}_{50}\text{Cu}_{50}$  alloy may be blocked by the martensitic zone in the as cast microstructure, and the shear position can be hindered by the growth of microcracks. The SEM image in Figure 5 (b) clearly indicates that the formation of serrated microcracks is achieved through continuous rotation of shear stress throughout the entire sample. Therefore, it can be considered that narrow-spacing shear bands with different angles propagating to the compression direction can prevent the propagation of microcracks.

The plasticity of the  $\text{Ti}_{50}\text{Cu}_{50}$  alloy can be controlled by the  $\gamma$ -TiCu phase. The strengthening of martensitic zone during the internal solidification process of TiCu matrix is observed. This martensitic zone plays an important role in changing the direction of local shear stress, and thus forms shear bands with different angles towards the direction of compressive load. It is believed that due to changes in local stress, jagged microcracks are formed, which serve as

a barrier that prevents their propagation in the sample. This means that when the sample is subjected to rotational shear stress, the formation of microcracks parallel to the compressive force can promote the macroscopic plasticity of the material.

#### 4. Conclusion

This article is devoted to  $\text{Ti}_{50}\text{Cu}_{50}$  as a research object; and TiCu alloy cast rod specimens were obtained by rapid solidification and copper mold vacuum suction casting method. Research has shown that in the  $\text{Ti}_{50}\text{Cu}_{50}$  alloy produced as cast rods, martensite was formed during rapid cooling, which was embedded as the  $\gamma$ -phase in the TiCu matrix. Local shear stress leads to rotational diffusion, interaction and strengthening of shear bands, resulting in good mechanical properties.

#### Acknowledgements

The work is partially supported by the Plan For Henan Provincial Department of education scientific research program(17A460027).

#### References

1. X. Zheng, C.C. Engler-Pinto, X. Su, H. Cui, W. Wen, *Materials Science and Engineering A*, **560**, 792, 2013.
2. Y.H. Kim, T.K. Ryou, H.J. Choi et al. *Journal of Material Processing Technology*, **123**, 270, 2002,
3. Beck T, Henne I, Löhe D., *Materials Science and Engineering A*, **483**, 382, 2008.
4. DHOuha M, HADDAR N, KOESTER A, et al., *Engineering Failure Analysis*, **45**, 85, 2014.
5. Liu W C, Radhakrishnan B, *Materials Letters*, **64**(16), 1829, 2010.
6. Beck T, Löhe D, Luft J, et al., *Materials Science and Engineering A*, 468, 184, 2007

7. Ola Jensrud, Ketill Pedersen. . *J. Material Processing Technology*, **80-81**,156, 1998.
8. Tangen S, Sjlstad K. Furu T. et al. *Metallurgical & Materials Transactions A*,**41**(11),: 2970, 2010.
9. Liu W, Ma M, Yang F. , *Metallurgical & Materials Transactions A*,**44**(6),2857, 2013.
10. Dubey S, Srivatsan T S, Socovelo W O., *International Journal of Fatigue*, **22**(2),161, 2000
11. **Zhao Yongqing**, *Alloys. Materials China*, **29**(5), 1-8 ??????
12. Ma Z Y, Mishra R S, Tjong S C. *Composite leta materialia*, **50**(17), 4293, 2002
13. Shang L M, Chen X P, Li X G, et al. . *Transactions of Materials & Heat Treatment*, **36**(6),78, 2015
14. **Zheng X. Engler-Pinto Jr C C. Su X. et al.** **Modeling of Fatigue Damage under Superimposed High-Cycle and ?????**
15. Stanzl-Tschegg S E, Meischel M. Arcari A, et al. *International Journal of Fatigue*,, **91**,352, 2016.
16. HU Qiyao, ZHAO Haidong, LI Fangdong. *J. Materials Science & Engineering: A*, **680**, 270, 2017,
17. ZUO P P, WU X C, ZENG Y, et al. *Fracture of Engineering Materials Structures*, **41**(1),59 2018.
18. LU Tiwen. SCUDION S. CHEN *Materials Science & Engineering A*,, **726**,126, 2018.
19. JIA Xiaoshuai, ZUO Xunwei, CHEN Nai, HUANG Jian, TANG Xinhua, RONG Yonghua. *Acta Metallurgica Sinica*. **49**(1), 35, 2013